Metakaryotic stem cell nuclei use pangenomic dsRNA/DNA intermediates in genome replication and segregation

William G Thilly[1,*], Elena V Gostjeva[1], Vera V Koledova[1], Lawrence R Zukerberg[2], Daniel Chung[3], Janna N Fomina[4], Firouz Darroudi[4], and B David Stollar[5]

[1]Laboratory in Metakaryotic Biology; Department of Biological Engineering; Massachusetts Institute of Technology; Cambridge, MA USA; [2]Department of Pathology; Massachusetts General Hospital; Boston, MA USA; [3]Gastrointestinal Unit; Massachusetts General Hospital; Boston, MA USA; [4]Department of Toxicogenetics; Leiden University Medical Centre; Leiden, The Netherlands; [5]Department of Developmental, Molecular and Chemical Biology; Tufts University School of Medicine; Boston, MA USA

Bell shaped nuclei of metakaryotic cells double their DNA content during and after symmetric and asymmetric amitotic fissions rather than in the separate, pre-mitotic S-phase of eukaryotic cells. A parsimonious hypothesis was tested that the two anti-parallel strands of each chromatid DNA helix were first segregated as ssDNA-containing complexes into sister nuclei then copied to recreate a dsDNA genome. Metakaryotic nuclei that were treated during amitosis with RNase A and stained with acridine orange or fluorescent antibody to ssDNA revealed large amounts of ssDNA. Without RNase treatment metakaryotic nuclei in amitosis stained strongly with an antibody complex specific to dsRNA/DNA. Images of amitotic figures co-stained with dsRNA/DNA antibody and DAPI indicated that the entire interphase dsDNA genome (B-form helices) was transformed into two dsRNA/DNA genomes (A-form helices) that were segregated in the daughter cell nuclei then retransformed into dsDNA. As this process segregates DNA strands of opposite polarity in sister cells it hypothetically offers a sequential switching mechanism within the diverging stem cell lineages of development.

Introduction

Cells with large, hollow, bell shaped nuclei arise at the time of organ bud appearance by symmetric amitosis of precursor embryonic cell nuclei in humans (4–7 wks of gestation), rodents and plants.[1-3] In humans and rodents the two bell shaped nuclei are soon encased in a sarcoplasmic tubular syncytium in which bell shaped nuclei increase by successive amitotic divisions up to 16 (brain) or 32 (colon) by symmetric amitoses. These large tubular syncytia themselves increase in number and are observed as groups of radio-spherical clusters within organ anlagen up to 12th-14th wks. The syncytial nuclei are then redistributed throughout the fetal organs as mononuclear cells in which each bell shaped nucleus is appended to, rather than enclosed in, a spheroidal to oblate spheroidal cytoplasmic organelle. During organogenesis both syncytial and mononuclear metakaryotic nuclei undergo asymmetric amitoses to form a highly diverse, tissue-specific set of at least nine morphologically distinguishable forms of closed, intra-cytoplasmic eukaryotic nuclei.[1] Some of the eukaryotic cells newly created by asymmetrical amitoses of the metakaryotic lineage increase by mitotic divisions to form the organized epithelium of solid tissues and tumors.[1-3]

Because these cells' cytology and behavior in nuclear fission differed markedly from eukaryotic cells and because they appeared to drive the growth and differentiation of post-embryonic meta-organs they have been denominated metakaryotes.[1] The cytological evidence of asymmetric nuclear fissions creating cells with eukaryotic nuclei that increase by mitoses to define the fetal/juvenile tissue or tumor parenchyma in humans supported the inference that cells with bell shaped nuclei comprise a stem cell lineage in organogenesis and carcinogenesis.[1,2] The nuclear bell shapes and arrays of eukaryotic nuclear forms seen in adenomatous and mesenchymal tumor areas are not easily distinguished from those in developing fetal organs of the second trimester.[1-3] Tubular syncytial metakaryotes have been reported as "myotubes," mononuclear metakaryotes with spherical oblate cytoplasmic organelles as "goblet cells" and mononuclear metakaryotes with near spherical cytoplasmic organelles as "signet ring cells."[3] These findings extend those dating to the early 19th century indicating that tumors display the growth rates and histologic characteristics of developing fetuses.[4]

Cytogenetic studies of the interphase metakaryotic nuclei indicated that all of their chromosomal centromeres and telomeres were paired and telomeres end-joined. Opening and reclosing of a small number of end-joined telomeric regions during the syncytial

phase of development (4–12 wks) have been inferred from three dimensional images in human syncytial metakaryotes.[5]

Quantitative cytometry of Feulgen stained nuclei found that bell shaped nuclei segregated and doubled their DNA content coordinately during and after amitotic fission.[3] Feulgen DNA images showed that these processes began with the appearance of two separate pairs of condensed DNA rings at the bell mouth increasing the total amount of DNA to 110% of the interphase DNA content. As the two separate pairs of double rings separated Feulgen DNA content monotonically increased to twice the diploid genomic complement.[3] DNA strands were somehow simultaneously segregated into two daughter nuclei and copied without loss of genomic information. A parsimonious hypothesis was that the anti-parallel + and – strands of the DNA helix were separated as pangenomic replicative intermediates containing single stranded DNA (ssDNA).

Results

To test this hypothesis we used acridine orange as a metachromatic stain for single (orange fluorescence) and double stranded (green fluorescence) nucleic acids in fetal tissue samples.

Closed nuclei contained within the cytoplasm of eukaryotic cells emitted strong green fluorescence expected of dsDNA-containing chromatin. Eukaryotic cell cytoplasms emitted strong orange fluorescence associated with the single-stranded rRNA of ribosomes.

The bell shaped nuclei of metakaryotic syncytia and mononuclear cells also displayed strong green fluorescence. Bright red fluorescence interpreted to be rRNA was observed between the bell shaped nuclei of some but not all syncytia (4–12 wks) and within the cytoplasmic organelles of mononuclear cells (12–16 wks).

Following RNase A treatment of fixed specimens to destroy interfering rRNA, orange fluorescence was not detected in cytoplasms of any eukaryotic or metakaryotic cells or syncytia. Removal of rRNA in syncytia required use of a high concentration of RNase A (2.0 mg/ml). Bell shaped nuclei in most metakaryotic syncytia in which nuclei were well-separated emitted green fluorescence. However, multiple orange nuclei were found in fetal samples containing tubular syncytia with closely paired bell shaped nuclei undergoing symmetrical amitotic fissions These images extended earlier observations indicating synchronous metakaryotic amitoses among and within fetal organs.[1,3] With RNase A pre-treatment, both "kissing bell" (**Fig. 1A–F**) and "stacked cup" (**Fig. 1G–J**) forms of amitotic fission figures were invariably found to strongly emit orange fluorescence.[3] Amitotic figures were observed in which the entire nuclear body emitted red-orange fluorescence (**Fig. 1F and J**). These images were interpreted as supportive of the hypothesis that metakaryotic amitoses somehow separated their genomes using ssDNA-containing complexes but the interpretation of orange fluorescence as ssDNA lacked sufficient specificity insofar as unknown substances might also have elicited the observations. See also **Figure S1**.
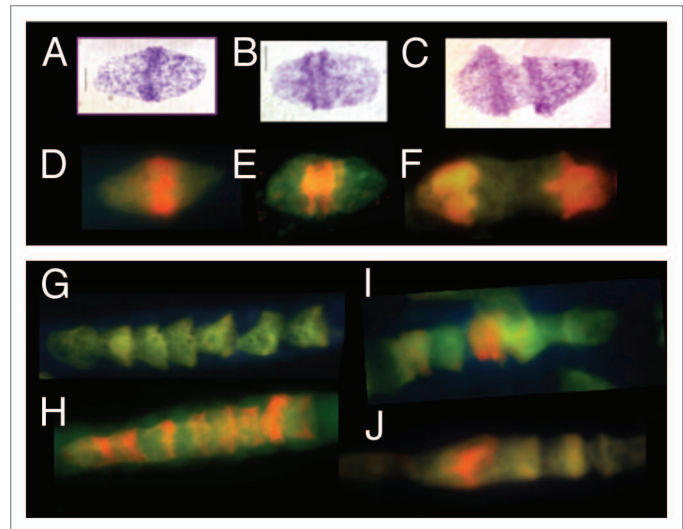
Figure 1. Metakaryotic nuclei undergoing two forms of symmetrical amitoses within tubular syncytia of fetal spinal cord ganglia (9 wks). (**A, B, and C**) Three "kissing bell" amitoses with DNA stained Feulgen reagent (purple). The order shown represents the stages of (**A**) formation of two pairs of condensed DNA rings at the rim of the bell mouth that (**B**) separate as total DNA increases and (**C**) proceeds toward complete separation when an exact doubling of DNA is observed.[3] (**D, E, and F**) Three "kissing bell" amitoses stained with acridine orange after treatment with RNase. The order shown represents the stages of (**D**) appearance of bright orange fluorescence co-localized with the condensed DNA rings of Feulgen stained condensed DNA as in (**A**), (**E**) separation of two orange rings at the bell mouths as total DNA increases as in (**B and F**) progress toward complete separation as in (**C**). (**G, H, I, and J**) Four lower magnification images of syncytia stained with acridine orange after RNase treatment. (**G**) A section of a syncytium with well-separated bell shaped nuclei showing the common "stacked cup" relationship of metakaryotic nuclei in tubular syncytia when no amitoses are evident. Well-separated bell shaped nuclei stained with acridine orange emit green fluorescence with scant amount of orange fluorescence. (**H**) A tubular syncytial section with bell shaped nuclei displaying the closely stacked nuclei indicative of synchronous amitoses and strong orange fluorescence associated in this example with the rims of the bell mouths. (**I and J**) Two syncytial sections displaying the "stacking cup" form of amitoses with varying degrees of separation between nuclei and the intensity and distribution of orange fluorescence among nuclei within the syncytia. *Images by EVG.*

Fluorescent antibody to ssDNA was thus used as an independent, more specific, diagnostic probe to test the interpretation that the orange fluorescence of RNase-treated metakaryotic nuclei during amitosis emanated specifically from ssDNA.[6] Images from RNase-treated preparations stained with acridine orange (**Fig. 2A, C, and E**) were compared with images stained with ssDNA monoclonal antibody, *Mab F7–26,* (**Fig. 2B, D, and E**). Both methods yielded evidence of large amounts of ssDNA-containing material throughout metakaryotic amitosis. Both methods indicated a synchronous ssDNA appearance within syncytia (**Fig. 2A and B**), early ssDNA appearance at the bell mouth (**Fig. 2C and D**), and ssDNA distributed throughout the body of bell shaped nuclei (**Fig. 2E and F**). It was clear that both methods of ssDNA recognition yielded the same distributions of fluorescence in all
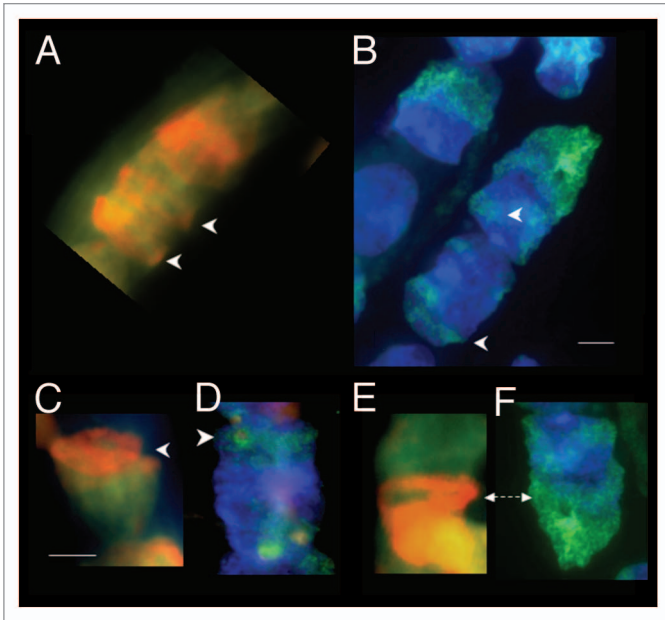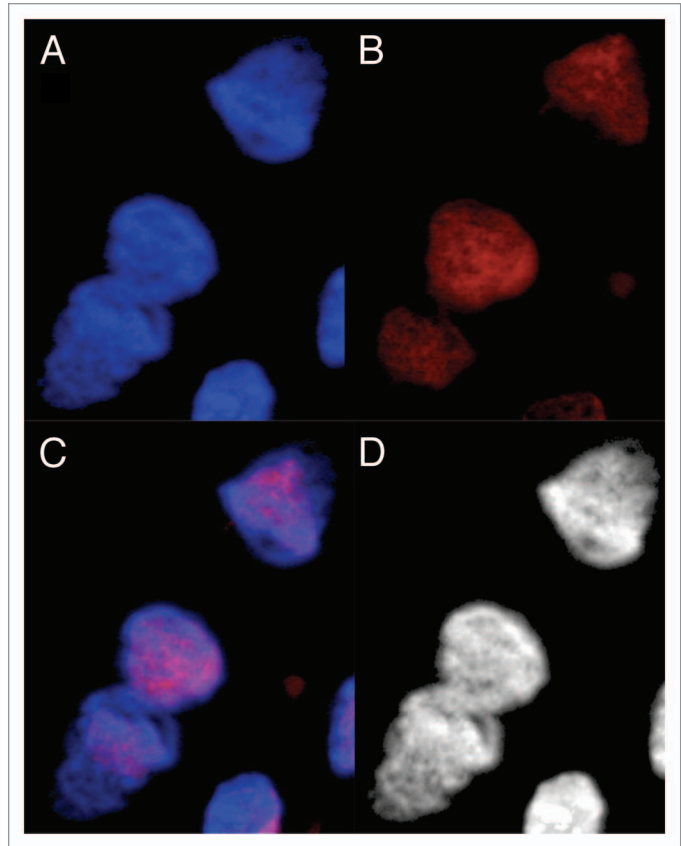
Figure 2. Fluorescent (FITC green) Mab F7–26 ssDNA antibody complex and acridine orange staining of RNase-treated syncytia within tubular syncytia of fetal spinal cord ganglia (9 wks). (**A, C, and E**) Acridine orange staining showing various spatial distributions of bright orange fluorescence in syncytial bell shaped nuclei. (**B, D, and F**) Anti-ssDNA labeling (FITC green) of bell shaped nuclei in the same samples with DAPI (blue) staining of dsDNA. Arrows emphasize the similarity of distribution of both modes of ssDNA recognition starting at the rim of the mouths of the nuclei. Scale bar, 5 μm. Images by Gostjeva EV, Fomina JN, and Darroudi F.

Figure 3. Images of dsDNA (DAPI, blue) and dsRNA/DNA (TRITC-Ab, red) stain in metakaryotic syncytial nuclei undergoing symmetric amitoses in fetal spinal cord, 10 wks. (**A**) DAPI fluorescence (blue). (**B**) TRITC-Ab fluorescence (red). (**C**) Merged images of (**A**) and (**B**) showing nuclei labeled simultaneously with DAPI and TRITC-Ab-n3. (**D**) Achromatic image of (**A**). Scale bar, 5 μm. Image by Koledova VV.

amitotic figures derived from RNase-treated specimens of fetal tissues and tumors. These observations permitted the inference that the metakaryotic amitotic fission figures contained large quantities of ssDNA-containing complex. See also **Figure S2**. It should be noted that no eukaryotic nuclei, including those in mitosis within these preparations yielded any signal suggestive of the presence of ssDNA within our limit of detection (< 1/1000 of a pangenomic equivalent).

Amitotic metakaryotic nuclei that were not RNase treated showed no indication of ssDNA suggesting that the ssDNA-containing complex was a dsRNA/DNA duplex. However, it was possible that RNase A treatment or other preparative steps had somehow converted a metakaryotic genomic replicative intermediate from a B to an A form of dsDNA helix or other novel form that might conceivably emit orange-red fluorescence in the presence of acridine orange and bind antibodies thought to be specific for ssDNA.

To test this possibility red-fluorescent antibody complexes specific for dsRNA/DNA duplexes were applied to samples that were not treated with RNase A: fetal tissues, adult tumors and a human colonic adenocarcinoma-derived line, HT-29.[7-9] Specimens were stained both with antibody to dsRNA/DNA and DAPI (4′, 6-diamidino-2-phenylindole), generally employed as a blue fluorescent dsDNA marker. The derived images (**Figs. 3 and** 4) indicated considerable amounts of a dsRNA/DNA-containing complex in all metakaryotic nuclei undergoing

amitotic fission. Neighboring eukaryotic nuclei were not labeled with dsRNA/DNA antibody save for small amounts, less than 0.1% relative to labeled amitotic metakaryotic nuclei, previously associated with transcription intermediates.[10-14] Specificity of the staining was tested and confirmed using low concentrations of soluble poly(A):poly(dT), an authentic RNA/DNA hybrid to inhibit the staining of metakaryotic amitotic figures by the dsRNA/DNA antibody. Importantly, dsRNA/DNA antibody did not bind to any nuclei in RNase-treated specimens, a finding consistent with the antibody's selectivity; it does not recognize ssDNA or dsDNA. Others have found that dsRNA/DNA exists predominantly in A form as opposed to the B form of dsDNA.[15,16] Together these observations indicated that amitotic figures in bell-shaped amitotic metakaryotic nuclei were associated with formation and segregation of dsRNA/DNA.

Bell shaped nuclei involved in symmetrical and asymmetrical amitotic fission in fetal tissue usually contained both strong DAPI and dsRNA/DNA antibody staining signals indicative of the simultaneous presence of dsDNA and dsDNA/RNA during the period of genome doubling and amitotic segregation. Some images of asymmetric amitoses, however, demonstrated nuclei heavily labeled with fluorescent dsRNA/DNA antibody without

any detectable blue fluorescence associated with dsDNA-bound DAPI, see **Figures S1–S9**.

Similarly to these observations in syncytia and mononuclear metakaryotic amitoses in fetal tissues, large amounts of dsRNA/DNA antibody stained material were found in metakaryotic amitotic figures of human tumors (**Fig. 5**; **Fig. S6 and S7**) and the human colonic adenocarcinoma-derived cell line, HT-29 (**Fig. 6**; **Figs. S8 and S9**).

Together these images of nuclei positive for dsRNA/DNA antibody binding but negative for DAPI staining show that some post amitotic nuclear genomes may be comprised entirely of dsRNA/DNA while containing no detectable dsDNA in human fetal, tumor and tumor derived cell line metakaryotic nuclei undergoing amitoses. No reference to specificity of DAPI for dsDNA (B-form) vs. dsRNA/DNA (A-form) has been found; it appears that this may be the first report of this interesting and potentially useful property.

That DAPI did not appear to stain dsRNA/DNA (A-form helix) recalled the use of Hoechst dyes employed by Sam Latt to distinguish between native dsDNA and dsDNA bifilarly substituted with bromodeoxyuridine for thymidine.[17] Such substitution has been reported to converted native B form into A-form dsDNA.[18]

That DAPI apparently did not stain nuclei with copious amounts of dsRNA/DNA also recalled the primary observation of Joe Gray that a Hoechst negative "side population" of rat bone marrow cells when isolated by fluorescence-activated cell sorting was remarkably enriched for stem cells as demonstrated by their ability upon transplant to recreate the entire hematoleukopoietic system.[19]

Seeking for some molecular marker relevant to our interpretation that a pangenomic dsRNA/DNA replicative intermediate the amitotic metakaryotic fission we noted that only one RNase in the human genome, RNase H-1, has been reported to have the quality of processive exonucleolyticX activity.[20] This activity could be used to rapidly remove the hypothesized RNA strand as it is replaced by a DNA strand in the post segregation nuclei. Furthermore, RNase H1 gene knockout mouse experiments discovered that embryonic development proceeded normally but development halted at the embryonic/fetal transition when metakaryotes first appear in mice and humans.[3,21] Accordingly we obtained antibody for this human enzyme and discovered that all metakaryotic nuclei in amitosis were heavily labeled while no signals could be detected from eukaryotic cells or metakaryotic nuclei that were not in amitoses (**Fig. S10**). Co-localization of antigen reacting with human RNase H-1 specific antibody with material hypothesized to be dsRNA/DNA was clearly evident in all preparations studied. The approach offers a general path for discovery of gene products expressed in metakaryotic amitotic figures. First, a gene is nominated as one required for metakaryotic cells but not eukaryotic cells if upon knockout in mice it blocks entry into the fetal period when the anlagen of meta-organs first appear. Second, antibodies for the gene product are applied to specimens containing both eukaryotic and metakaryotic cells including cells in mitosis or amitosis to discover if specific localization in metakaryotic amitotic fission figures is observed.
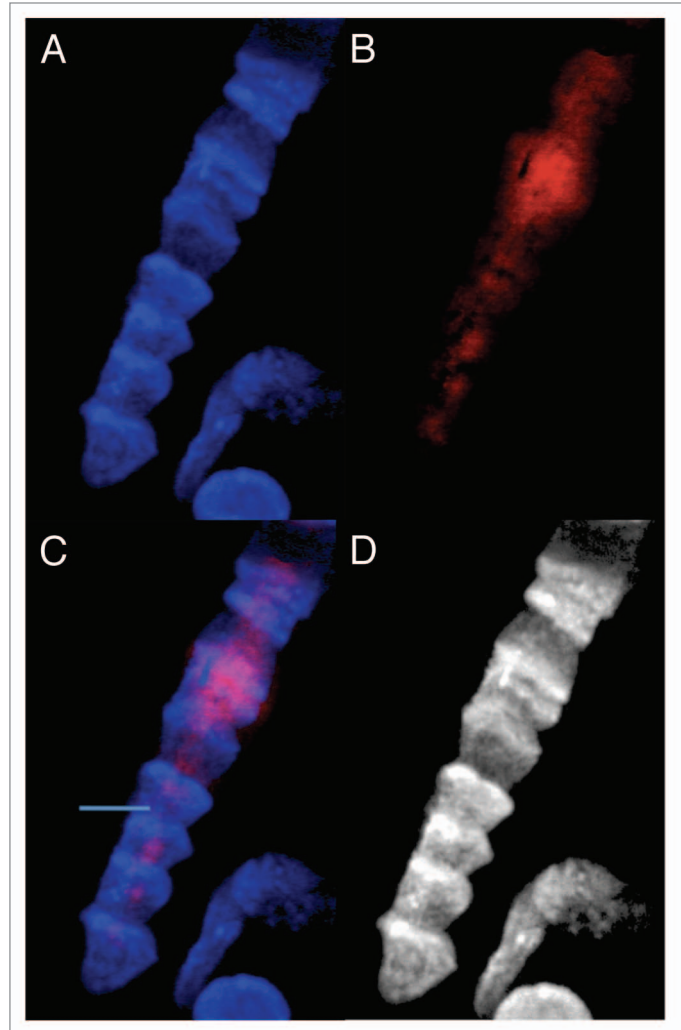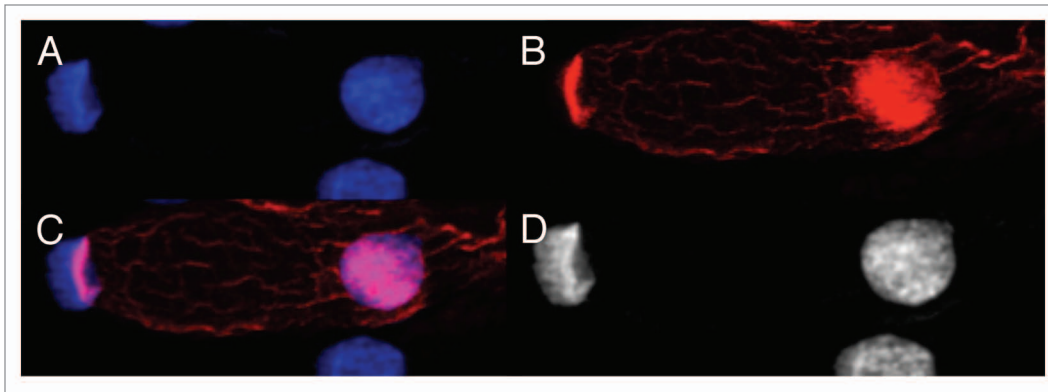

Figure 4. Images of dsDNA (DAPI, blue) and dsRNA/DNA (TRITC-Ab, red) stain in metakaryotic syncytial nuclei undergoing synchronous symmetrical amitoses in fetal spinal cord, 10 wks. (**A**) DAPI fluorescence (blue). (**B**) TRITC-Ab fluorescence (red). (**C**) Merged images of (**A**) and (**B**) showing nuclei labeled simultaneously with DAPI and TRITC-Ab. (**D**) Achromatic image of (**A**). Image by Koledova VV.

Discussion

This is not the first report of a dsRNA/DNA genomic replicative intermediate in human cells. Priority belongs to those students of the eukaryotic cell mitochondrial genome who have previously used dsRNA/DNA antibody and molecular separations to reveal dsRNA/DNA replicative intermediates in which RNA synthesis on a DNA template represents DNA strand displacement followed by RNase digestion and DNA copying.[22,23]

This, however, appears to be the first report of a nuclear dsRNA/DNA pangenomic replicative intermediate in human or any other metazoan cell. Extensive amounts of dsRNA/DNA intermediates comprising ~10–100% of the genomic mass were found in all metakaryotic bell-shaped nuclei undergoing amitotic divisions in human fetal tissues, tumors and the tumor

Figure 5. Images of dsDNA (DAPI, blue) and dsRNA/DNA (TRITC-Ab, red) stain in mononuclear metakaryotic cell undergoing asymmetrical amitosis in a colonic adenocarcinoma (M, 68 y). (**A**) DAPI fluorescence (blue). (**B**) TRITC-Ab fluorescence (red). (**C**) Merged images of (**A and B**) showing nuclei labeled simultaneously with DAPI and TRITC-Ab. (**D**) Achromatic image of (**A**). Image is interpreted as an asymmetrical amitosis in which both parent bell shaped nucleus and daughter spherical nucleus have reconverted a large fraction of the dsRNA/DNA intermediate (red) to the dsDNA form (blue). Appearance of red fragments or striations of dsRNA/DNA antibody labeling in cytoplasmic volume between nuclei is occasionally observed as shown here in tumors and in the HT-29 cell line. Image by Koledova VV.

cell line HT-29 (**Figs. 1–6**; **Figs. S1–S9**). No indications of extensive dsRNA/DNA intermediates (<0.01%) were observed in eukaryotic cells of any preparation; these small signals may be attributed to transient RNA/DNA transcription duplexes.[13]

The metachromatic dye acridine orange and the fluorescent antibody to ssDNA indicated the presence of large amounts of ssDNA in amitotic nuclei in RNase-treated but not untreated preparations (**Figs. 1 and 2**). Fluorescent antibody specific to dsRNA/DNA provided direct evidence that the amitotic fission figures contained large amounts of dsRNA/DNA (**Figs. 3–5**). Importantly, RNase treated preparations were not labeled by antibody to dsRNA/DNA.

This is not a minor point: it was conceivable that antibodies raised against authentic dsRNA/DNA or authentic dsDNA bifilarly substituted with bromodeoxyuridine that assume the A-form of nucleic acid helices recognize the epitopes of A-form helices and not dsRNA/DNA specifically. But such complexes would not also be degraded by RNase treatment.

The images indicate that synthesis of dsRNA/DNA replicative intermediate began in the condensed DNA rings of the metakaryotic bell mouth, continued through the bulk of the nuclear DNA during nuclear segregation. This pattern accords with the increases in dsDNA observed by quantitative Feulgen cytometry during and/or after nuclear fission (**Figs. 1–4**).[3]

Furthermore, nuclei in some metakaryotic amitotic nuclear fission figures were negative for DAPI staining and positive for dsRNA/DNA fluorescent antibody staining (HT-29 cells, **Figs. S3 and S4**)**.** These images indicated that DAPI, which causes dsDNA to fluoresce brightly, does not cause the dsRNA/DNA to fluoresce. As dsDNA is predominantly of the B-form of helix and dsRNA/DNA of the A-form it appears that DAPI differentiates between the interphase dsDNA and the dsRNA/DNA of the metakaryotic amitotic genomic replicative intermediate.[15] As noted above, images in which one nucleus is labeled with antibody for dsRNA/DNA but negative for DAPI, e.g., **Figure S9**, indicate that the entire dsDNA genome can be
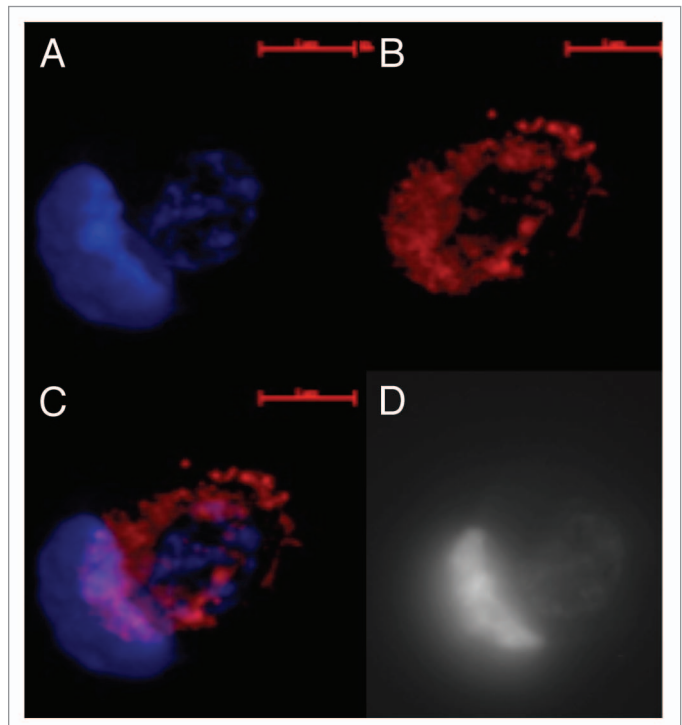
Figure 6. Image of dsDNA (DAPI, blue) and dsRNA/DNA (TRITC-Ab, red) in mononuclear metakaryotic nucleus undergoing asymmetrical amitosis in the HT-29 cell line. (**A**) DAPI fluorescence (blue). (**B**) TRITC-Ab fluorescence (red). (**C**) Merged images of (**A and B**) showing nuclei labeled simultaneously with DAPI and TRITC-Ab. (**D**) Achromatic image of (**A**). This figure is interpreted pro tempore as an asymmetric form of amitosis: parent bell shaped nucleus has been reconverted to dsDNA (blue) without any indication of dsRNA/DNA (red) but in the derived oval nucleus a substantial fraction of the dsRNA/DNA intermediate (red) has been reconverted to dsDNA (blue) during nuclear segregation which is not yet completed in this example. Asymmetrical cell division is a characteristic expected of a stem cell. Image by Koledova VV.

converted to the dsRNA/DNA form. Most images so labeled indicate that the process of reconversion from the dsRNA/DNA form to dsDNA form can begin prior to complete separation of the sister nuclei.[3]

However, the suggested interpretation of these observations portends a major paradigm shift in understanding genome replication in human organogenic, carcinogenic and other stem cells. It is thus important to consider other possibilities than the one we have advanced.

One may conjecture that the epitopes recognized by antibody raised against RNA/DNA duplexes might recognize any A-form of nucleic acid duplex and not be specific for dsRNA/DNA alone. However, it is clear that the duplex observed is degraded by RNase A permitting the conclusion that the duplex contains reasonably extensive amounts of ribonucleotides. This said, one may note that it has not been proven that the predominantly "RNA" sequence of the hypothesized dsRNA/DNA duplex is comprised of RNA alone. If it were a mixed polymer with both RNA and DNA variable stretches (dsXNA/DNA) the duplex might conceivably be converted to a predominantly A-form and still be considerably degraded by both RNase A in fixed specimens and human RNase H1 in live cells. As such it might not fluoresce in the presence of DAPI or Hoechst dyes.

Biophysical methods clearly need to be applied in future research so that the dsRNA/DNA complexes and auxiliary macromolecules associated with them may be studied as in studies of eukaryotic dsRNA/DNA mitochondrial genome replication intermediates.[20-23] But the low fraction of metakaryotic cells in fetal tissues and tumors that are undergoing amitoses (<1/10 000) presents a challenge to such studies. Transcriptional dsRNA/DNA intermediates encompassing ~1/10 000 to 1/1000 of the interphase genome in the vast majority of growing eukaryotic cells would constitute an unacceptable level of background "noise." Isolation of metakaryotes in amitosis presents additional technical challenges: low numbers and their rapid creation of new eukaryotic nuclei as products of asymmetric amitoses that comprise most of the amitotic divisions in fetal/juvenile organ and tumor growth.[1-3]

This said, the images presented demonstrate that metakaryotic cell nuclei undergoing symmetric or asymmetric amitosis can be identified in fixed preparations by fluorescent antibodies specific for dsRNA/DNA or RNase H1, by acridine orange fluorescence or binding of ssDNA-specific antibody in RNase treated specimens. They may also be identified by the absence of fluorescence in bell shaped nuclei treated with DAPI or any other dye that distinguishes between A and B form nucleic acid double strand helices in fixed or live cells, e.g., dsRNA/DNA and dsDNA, respectively. The observations are readily reproduced using, for example, HT-29 cells available from the American Type Culture Collection, the commonly available reagents, RNase A, acridine orange, DAPI and a fluorescence microscope.

We have interpreted the images of metakaryotic symmetric and asymmetric divisions during growth and differentiation in fetal tissues and tumors as evidence that they comprise a significant portion of their respective stem cell lineages.[1-3] Subject to the caveats mentioned above, observations leading to the interpretation that dsRNA/DNA is found in each amitotic division of the metakaryotic lineage naturally provokes the thought that dsRNA/DNA may be an essential structural component of developmental machinery. Note that these observations have not differentiated among possible pairings of + and – strands of parental DNA copies in each daughter cell. As information from both parental chromatids is found in individual human tissue and tumor cells it appears that each daughter stem cell has received a ssDNA copy from both the maternal and the paternal dsDNA copies of the parent cell. Given this restraint the possible pairings of maternal (+/-) and paternal (+/-) ssDNA copies of any genomic subsequence are four: m+/p+, m+p-, m-p+ and m-p-.

This apparent segregation of anti-parallel genomes in metakaryotic stem cells was anticipated by the observation almost 50 y ago that sister chromatids in mouse embryonic primary cell culture were non-randomly co-segregated in successive divisions.[24] Cairns cited this work in forming his hypothesis of an "immortal strand" of DNA in adult maintenance stem cells of epithelial tissues such as in the colon.[25] Importantly, Sherley and his coworkers have specifically demonstrated pangenomic co-segregation of bromodeoxyuridine containing DNA strands and chromatin associated hydroxy-methyl cytosine in cultured fetal mouse cells undergoing successive asymmetric divisions.[26,27]

Subsequent studies of early mouse development have provided definitive evidence of developmental switches at the genomic level. Developmental steps in the mitotic, eukaryotic pre-fetal embryonic stem cell divisions are accompanied by non-random chromatid segregations.[28-30] The first appearance of metakaryotic stem cells, derived from previously eukaryotic embryonic stem cell precursors seems to mark the beginning of fetal development in mice and humans.[3] Their segregation of information embodied in parental + and – chromatid strands via dsRNA/DNA replicative intermediates suggests a mechanistic element of fetal developmental switching.

The "diploid" genome may in this sense be considered to contain, not two, but four different pangenomic sets of information. Any asymmetric distribution of epigenetic factors in stem cell genomes would presumably undergo segregation during developmental doublings and could represent binary switches.[31] Programmed sequential dissociations of imprinted information might be also be accomplished via the opening and closing of the circular "oligo-chromosomal" elements that appear to comprise the metakaryotic interphase genome.[5] A relatively small number of either of such events, e.g., fewer than 45, would be sufficient to uniquely specify each and every cell in human fetal through adult development.

Other possibilities related to dsRNA/DNA replicative intermediates abound. They may explain in part the mutator/hypermutable phenotype of human stem cells' mitochondrial and nuclear genomes in organogenesis and carcinogenesis.[23,32,33] The absence of an opposite DNA strand during post segregation DNA copying forces recognition that mismatch repair processes that severely reduce mutation rates in eukaryotic S-phase would not be available to metakaryotes. A nucleus in which large amounts of ribonucleotides are being freed by RNA degradation

by RNase H1 may be expected to erroneously incorporate some of them in DNA copying, depending on the particular DNA polymerases employed.

The presence of antibodies to dsRNA/DNA in sera of patients with the autoimmune disease systemic lupus erythrematosus may indicate the presence of unusually placed or disintegrating metakaryotic cells.[34,35] Metakaryotes in normal adult tissue may be the cells in which certain RNA viruses replicate by "hijacking" the metakaryotic machinery of dsRNA/DNA formation. This possibility may serve as the basis for directed anti-viral therapies.[36,37] The processes described peculiar to metakaryotic stem cells in division offer an array of targets for diagnosis and drug therapy in cancers and other diseases in which metakaryotic cells appear to comprise a stem cell lineage.

The characteristics peculiar to fetal/juvenile metakaryotic stem cells that differentiate them from embryonic eukaryotic stem cells now include: (1) large, open-mouthed, hollow, bell shaped nuclei appended to, rather than enclosed in, a cytoplasmic organelle in mononuclear metakaryotic cells,[1] (2) asymmetrical amitotic nuclear fissions that give rise to the mitotic eukaryotic cells of fetal/juvenile tissues and their derived tumors.[1,2] (3) pangenomic homologous centromeric/telomeric pairing end-to-end telomeric joining,[5] (4) DNA increase concomitant with genomic segregation,[3] (5) pangenomic dsRNA/DNA nuclear replication intermediates associated with large amounts of RNase H1, and (6) a mutator/hypermutable phenotype limited to the fetal juvenile period sufficient to account for the age-specific human experience of colorectal cancer.[32,38]

Their presence in developing rodents and plants indicates an evolutionary origin that, like mitochondria, predates the separation of plant and animal kingdoms.[3] The metakaryotic nuclear morphology and processes of genomic segregation and replication are clearly different from those found in mitotic eukaryotic cellular forms of yeast, insect and mammalian cells. It would be prudent to explore these newly discovered but ubiquitous, metakaryotic, forms of life more deeply in order to better understand their roles in human development and defeat their roles in related pathologies. It would also be prudent to imagine and search for other stem cell forms.

Materials and Methods

Tissue and tumor samples

All human anonymous surgical discard samples were obtained under a protocol approved in advance by the MIT Committee on the Use of Humans as Experimental Subjects and the IRBs of each contributing hospital. Anonymous surgical discards were fixed immediately upon surgical removal in Carnoy's solution as described and stored under refrigeration in 70% ethanol.[1] Fetal tissues of hindgut, spinal cord and rib cage muscle were used for the cytometric analyses reported here. Tumor samples were obtained from adults.

Source and maintenance of HT-29 cell line

The HT-29 cell line was created from the colonic adenocarcinoma of a 44 y old female by the late Jorgen Fogh and deposited by him in the 1970s in the American Type Tissue Collection (ATCC).[2] Frozen aliquots in the 38th passage were purchased from the ATCC (HTB-38™) under a Material Transfer Agreement stipulating limitation to non-commercial use. Cells of this "38th passage" were then propagated for > 2 years in 25 cm^2 T-flasks with weekly passages of 16 000 trypsinized cells which grew to near confluence (0.5–1 million total cells) in the seven days between passages. Cells were grown in MEM medium (GIBCO) modified to our specification to be free of antibiotics, sodium bicarbonate and glucose but containing 10 mM fructose. Closed flasks were placed in a 37 °C incubator under ambient atmospheric conditions. Regular independent assays for mycoplasma were all negative.

Slide preparation

Fixed ~5–7 mm^3 tissue/tumor solid tissues were enzymatically dissociated in collagenase II (10 U/μl) (Life Technologies) and spread on microscopic slides as cells monolayers.[1] Briefly, samples were cut into ~2 mm^3 pieces, placed in 2 ml tubes filled with collagenase II, 37 °C, and digested for 2 h (tumor tissues) or 45 min (fetal tissues). The resulting digested tissue pieces were rinsed in distilled water, placed in 45% acetic acid for 15 min (maceration) and then applied to slides for spreading. Slides were frozen on dry ice, coverslips removed, and dried at room temperature.[1,3]

HT-29 cells were fixed directly in T-flasks or on microscope slides. HT-29 cells were also observed live using phase contrast optics and/or fluorescence microscopy.

Histochemical staining

Feulgen staining

Dry slides were stained in Schiff's reagent (Sigma-Aldrich Inc.) for 1 h, rinsed twice in 2× SSC buffer (trisodium citrate 8.8 g/L, sodium chloride 17.5 g/L), stained in Giemsa (azure-eosin-methylene blue solution for microscopy) (Electron Microscopy Sciences Inc.). 1% Giemsa solution is concentrated Giemsa diluted in Sörenssen's buffer (disodium hydrogen phosphate dihydrate 11.87 g/L, potassium dihydrogen phosphate 9.07 g/L). Following the rinse in 2XSSC buffer slides were stained in 1% Giemsa for 5 min, then rinsed quickly once in Sörenssen buffer, then in running distilled water and then air-dried. Dry slides were placed in Xylene for 3 h before coverslips were glued with DePex mounting media (*Electron Microscopy Sciences*).

Acridine orange staining

Prior to staining with acridine orange freshly prepared tissue spread slides were exposed to RNase A (LifeTechnologies) for two hours at 37 °C in phosphate buffered saline. A notably higher RNase concentration, 2 mg/ml, than has been reported for eukaryotic cells was required for complete digestion of presumptive rRNA in mononuclear and especially syncytial metakaryotic cytoplasms.[34] A drop of RNase solution was placed directly on a top of cell spreads, covered with a coverslip and wrapped in paraffin paper and placed in a 37 °C incubator. Slides were washed in EDTA for 1 min, rinsed in molecular grade water and immediately stained in a Coplin jar at room temperature for 30 min with acridine orange solution. Acridine orange solution is 10 mg/ml solution in molecular grade water (Life Technologies) diluted in 500.0 ml distilled water and 5.0 ml of acetic acid adjusted to pH 3.1–3.4 (work solution, kept dark*).* Slides were

then successively rinsed in 0.5% acetic acid- ethanol, 100% ethanol and PBS then examined while still wet and covered with a coverslip.

DAPI and Hoechst 33258 staining

DAPI (Santa Cruz Biotechnology, Inc.) was used to recognize dsDNA in samples analyzed by immunofluorescence. For DAPI staining the fixed macerated tissue or cell samples were exposed to DAPI (0.3 micromolar in PBS) for 1–5 min at room temperature followed by three five-minute washes with cold 1× PBS wash buffer. Hoechst 33258 (Enzo Life Sciences) was applied from a stock solution to cell culture media at a final concentration of 1.0 micromolar.

Immunohistochemical staining

ssDNA antibody staining

The monoclonal antibody (Mab) F7–26 was used for detecting ssDNA intermediates (Bender MedSystems GmbH, Vienna, Austria) immediately after RNase A treatment as described above. This reagent is used commonly to detect ssDNA after brief boiling of specimens to detect short denaturable DNA strands in apoptotic cells. We followed the directions of the supplier save for amendment (WGT) by omission of the brief boiling step as we were seeking to detect ssDNA in RNase treated, non-apoptotic cells. The stock solution of antibody was diluted 10× with PBS and 5% fetal bovine serum immediately before use. A series of washing steps was performed prior to applying ssDNA antibody, using 0.005% pepsin in 10 mM, HCl 50 mM $MgCl_2$ and 1% formaldehyde in 50 mM $MgCl_2$. Slides were washed 3× with PBS (5 min each). Finally, slides were washed with 0.05% Tween (Sigma-Aldrich), then with blocking protein 3% BSA in Tween and again in 0.05% Tween. Afterwards, slides were treated with Mab F7–26 in 5% FBS for 60 min at room temperature, followed by application of anti-mouse Ig-G-FITC, Alexa 488 for 30 min. For co-staining with DAPI, slides were dehydrated in a series of ethanol, 70%, 90%, and 100% solutions, air-dried and mounted in "Citifluor" media (Citifluor Ltd.)

dsRNA/DNA specific antibody staining

Polyclonal dsRNA/DNA-specific antibodies obtained from a goat immunized with poly(A):poly(dT):methylated BSA complexes were used in observations of fetal and tumor tissues and HT-29 cells (BDS laboratory). Serum IgG, purified by DEAE-cellulose chromatography, was passed through poly(A)-cellulose and poly(dT)-cellulose columns to remove antibody cross-reactive with single stranded nucleic acids, and antibody reacting with dsRNA was removed by precipitation with poly(A):poly(U). The remaining antibodies were highly selective for the dsRNA/DNA structure.[7] In practice a solution containing 0.05 to 0.12 mg/ml of IgG was applied to each slide. Competition experiments with authentic dsRNA/DNA duplexes were undertaken to test the specificity of the observed immunofluorescent staining. Low concentrations of exogenous poly(A):poly(dT) suppressed the binding of antibody to metakaryotic nuclei in amitosis, whereas similar concentrations of the dsRNA polymer poly(A):poly(U), dsDNA or ssDNA did not.

Human RNase H1 specific antibody staining

Fixed and macerated tissue was permeabilized with 0.1% Triton X-100 in 1× PBS for 5 min at room temperature and then washed twice with 1× PBS. Blocking solution was applied for 30 min at room temperature. All antibodies were obtained from Santa Cruz Biotechnology, Inc. and handled as recommended by the supplier. Primary antibodies against RNase H1 were diluted to a working concentration (1:250) in blocking solution, and tissue samples were incubated overnight with the primary antibodies at +4C and then washed three times (5–10 min each) with 1× PBS wash buffer. Secondary antibodies (TRITC-conjugated, Santa-Cruz) in 1× PBS were diluted immediately prior to use and incubated for 30–60 min at room temperature and then washed three times (5 min per wash) with 1× PBS wash buffer.

Microscopy and image analysis

Images were obtained using "AxioVision" software supporting "Axioscop 2 MOT" and "Imager Z1" microscopes (Carl Zeiss Gmbh). Images were transmitted from microscopes using planar apochromatic objectives. One microscope is equipped with an *ApoTome* sliding 3D module to provide three-dimensional images. Transmitted light (bright microscopy) was used when Feulgen stain alone was employed. A blue transmittance filter (460–502 nm) excitation waveband maximum was used for imaging of acridine orange stained cells. Acridine orange, a metachromatic dye, has two emission maxima at 525 nm and 650 nm (green and red respectively).

Supplemental Materials

Supplemental materials may be found here:
www.landesbioscience.com/journals/organogenesis/article/27684

References

1. Gostjeva EV, Zukerberg L, Chung D, Thilly WG. Bell-shaped nuclei dividing by symmetrical and asymmetrical nuclear fission have qualities of stem cells in human colonic embryogenesis and carcinogenesis. Cancer Genet Cytogenet 2006; 164:16-24; PMID:16364758; http://dx.doi.org/10.1016/j.cancergencyto.2005.05.005

2. Gostjeva EV, Thilly WG. Stem cell stages and the origins of colon cancer: a multidisciplinary perspective. Stem Cell Rev 2005; 1:243-51; PMID:17142861; http://dx.doi.org/10.1385/SCR:1:3:243

3. Gostjeva EV, Koledova V, Tomita-Mitchell A, Mitchell M, Goetsch MA, Varmuza S, Fomina JN, Darroudi F, Thilly WG. Metakaryotic stem cell lineages in organogenesis of humans and other metazoans. Organogenesis 2009; 5:191-200; PMID:20539738; http://dx.doi.org/10.4161/org.5.4.9632

4. Sell S. Stem cell origin of cancer and differentiation therapy. Crit Rev Oncol Hematol 2004; 51:1-28; PMID:15207251; http://dx.doi.org/10.1016/j.critrevonc.2004.04.007

5. Gruhl AN, Gostjeva EV, Thilly WG, Fomina JN, Darroudi F. Human fetal/tumor metakaryotic stem cells: pangenomic homologous pairing and telomeric end-joining of chromatids. Cancer Genet Cytogenet 2010; 203:203-8; PMID:21156234; http://dx.doi.org/10.1016/j.cancergencyto.2010.08.015

6. Fujita K, Kawarada Y, Terada K, Sugiyama T, Ohyama H, Yamada T. Quantitative detection of apoptotic thymocytes in low-dose X-irradiated mice by an anti-single-stranded DNA antibody. J Radiat Res 2000; 41:139-49; PMID:11037581; http://dx.doi.org/10.1269/jrr.41.139

7. Stollar BD. Doubls-helical polynucleotides: immunochemical recognition of differing conformations. Science 1970; 169:609-11; PMID:5426785; http://dx.doi.org/10.1126/science.169.3945.609

8. von Kleist S, Chany E, Burtin P, King M, Fogh J. Immunohistology of the antigenic pattern of a continuous cell line from a human colon tumor. J Natl Cancer Inst 1975; 55:555-60; PMID:1159834

9. Kitagawa Y, Stollar BD. Comparison of poly(A).poly(dT) and poly(I).poly(dC) as immunogens for the induction of antibodies to RNA-DNA hybrids. Mol Immunol 1982; 19:413-20; PMID:6178964; http://dx.doi.org/10.1016/0161-5890(82)90207-3

10. Rudkin G, Stollar B. Naturally occurring DNA/RNA hybrids. I. Normal patterns in polytene chromosomes. ICN-UCLA Symp. Mol Cell Biol 1977; 7:257-69

11. Büsen W, Amabis J, Leoncini O, Stollar B, Lara F. Immunofluorescent characterization of DNA-RNA hybrids on polytene chromosomes of Trichosia pubescens (Diptera, sciaridae). Chromosoma 1982; 87:247-62; PMID:6186442; http://dx.doi.org/10.1007/BF00327628

12. Alcover A, Izquierdo M, Stollar D, Kitagawa Y, Miranda M, Alonso C. In situ immunofluorescent visualization of chromosomal transcripts in polytene chromosomes. Chromosoma 1982; 87:263-77; PMID:6186443; http://dx.doi.org/10.1007/BF00327629

13. Testillano PS, Gorab E, Risueño MC. A new approach to map transcription sites at the ultrastructural level. J Histochem Cytochem 1994; 42:1-10; PMID:7505298; http://dx.doi.org/10.1177/42.1.7505298

14. Wei T, Baiqu H, Chunxiang L, Zhonghe Z. In situ visualization of rDNA arrangement and its relationship with subnucleolar structural regions in Allium sativum cell nucleolus. J Cell Sci 2003; 116:1117-25; PMID:12584254; http://dx.doi.org/10.1242/jcs.00323

15. Broyde S, Hingerty B. 'A' forms of RNAs in single strands, duplexes and RNA-DNA hybrids. Nucleic Acids Res 1978; 5:2729-41; PMID:693318; http://dx.doi.org/10.1093/nar/5.8.2729

16. Plumbridge TW, Brown JR. The interaction of adriamycin and adriamycin analogues with nucleic acids in the B and A conformations. Biochim Biophys Acta 1979; 563:181-92; PMID:497208; http://dx.doi.org/10.1016/0005-2787(79)90019-4

17. Latt SA. Localization of sister chromatid exchanges in human chromosomes. Science 1974; 185:74-6; PMID:4134970; http://dx.doi.org/10.1126/science.185.4145.74

18. Miki K, Shimizu M, Fujii M, Hossain MN, Ayusawa D. 5-Bromouracil disrupts nucleosome positioning by inducing A-form-like DNA conformation in yeast cells. Biochem Biophys Res Commun 2008; 368:662-9; PMID:18258180; http://dx.doi.org/10.1016/j.bbrc.2008.01.149

19. Pallavicini MG, Summers LJ, Dean PN, Gray JW. Enrichment of murine hemopoietic clonogenic cells by multivariate analyses and sorting. Exp Hematol 1985; 13:1173-81; PMID:4065264

20. Gaidamakov SA, Gorshkova II, Schuck P, Steinbach PJ, Yamada H, Crouch RJ, Cerritelli SM. Eukaryotic RNases H1 act processively by interactions through the duplex RNA-binding domain. Nucleic Acids Res 2005; 33:2166-75; PMID:15831789; http://dx.doi.org/10.1093/nar/gki510

21. Cerritelli SM, Frolova EG, Feng C, Grinberg A, Love PE, Crouch RJ. Failure to produce mitochondrial DNA results in embryonic lethality in Rnaseh1 null mice. Mol Cell 2003; 11:807-15; PMID:12667461; http://dx.doi.org/10.1016/S1097-2765(03)00088-1

22. Yang MY, Bowmaker M, Reyes A, Vergani L, Angeli P, Gringeri E, Jacobs HT, Holt IJ. Biased incorporation of ribonucleotides on the mitochondrial L-strand accounts for apparent strand-asymmetric DNA replication. Cell 2002; 111:495-505; PMID:12437923; http://dx.doi.org/10.1016/S0092-8674(02)01075-9

23. Pohjoismäki JL, Holmes JB, Wood SR, Yang MY, Yasukawa T, Reyes A, Bailey LJ, Cluett TJ, Goffart S, Willcox S, et al. Mammalian mitochondrial DNA replication intermediates are essentially duplex but contain extensive tracts of RNA/DNA hybrid. J Mol Biol 2010; 397:1144-55; PMID:20184890; http://dx.doi.org/10.1016/j.jmb.2010.02.029

24. Lark KG, Consigli RA, Minocha HC. Segregation of sister chromatids in mammalian cells. Science 1966; 154:1202-5; PMID:5921389; http://dx.doi.org/10.1126/science.154.3753.1202

25. Cairns J. Mutation selection and the natural history of cancer. Nature 1975; 255:197-200; PMID:1143315; http://dx.doi.org/10.1038/255197a0

26. Merok JR, Lansita JA, Tunstead JR, Sherley JL. Cosegregation of chromosomes containing immortal DNA strands in cells that cycle with asymmetric stem cell kinetics. Cancer Res 2002; 62:6791-5; PMID:12460886

27. Huh YH, Cohen J, Sherley JL. Higher 5-hydroxymethylcytosine identifies immortal DNA strand chromosomes in asymmetrically self-renewing distributed stem cells. Proc Natl Acad Sci U S A 2013; 110:16862-7; PMID:24082118; http://dx.doi.org/10.1073/pnas.1310323110

28. Armakolas A, Klar AJ. Cell type regulates selective segregation of mouse chromosome 7 DNA strands in mitosis. Science 2006; 311:1146-9; PMID:16497932; http://dx.doi.org/10.1126/science.1120519

29. Armakolas A, Klar AJ. Left-right dynein motor implicated in selective chromatid segregation in mouse cells. Science 2007; 315:100-1; PMID:17204651; http://dx.doi.org/10.1126/science.1129429

30. Armakolas A, Koutsilieris M, Klar AJ. Discovery of the mitotic selective chromatid segregation phenomenon and its implications for vertebrate development. Curr Opin Cell Biol 2010; 22:81-7; PMID:20022232; http://dx.doi.org/10.1016/j.ceb.2009.11.006

31. Vu TH, Li T, Nguyen D, Nguyen BT, Yao XM, Hu JF, Hoffman AR. Symmetric and asymmetric DNA methylation in the human IGF2-H19 imprinted region. Genomics 2000; 64:132-43; PMID:10729220; http://dx.doi.org/10.1006/geno.1999.6094

32. Sudo H, Li-Sucholeiki XC, Marcelino LA, Gruhl AN, Herrero-Jimenez P, Zarbl H, Willey JC, Furth EE, Morgenthaler S, Coller HA, et al. Fetal-juvenile origins of point mutations in the adult human tracheal-bronchial epithelium: absence of detectable effects of age, gender or smoking status. Mutat Res 2008; 646:25-40; PMID:18824180; http://dx.doi.org/10.1016/j.mrfmmm.2008.08.016

33. Ji J, Ng SH, Sharma V, Neculai D, Hussein S, Sam M, Trinh Q, Church GM, McPherson JD, Nagy A, et al. Elevated coding mutation rate during the reprogramming of human somatic cells into induced pluripotent stem cells. Stem Cells 2012; 30:435-40; PMID:22162363; http://dx.doi.org/10.1002/stem.1011

34. Talal N, Gallo RC. Antibodies to a DNA:RNA hybrid in systemic lupus erythematosus measured by a cellulose ester filter radioimmunoassay. Nat New Biol 1972; 240:240-2; PMID:4509164; http://dx.doi.org/10.1038/newbio240240a0

35. Alam K, Ali R. Human autoantibody binding to multiple conformations of DNA. Biochem Int 1992; 26:597-605; PMID:1376994

36. Yahi N, Baghdiguian S, Bolmont C, Fantini J. Replication and apical budding of HIV-1 in mucous-secreting colonic epithelial cells. J Acquir Immune Defic Syndr 1992; 5:993-1000; PMID:1280683

37. Eriksson M, Guse K, Bauerschmitz G, Virkkunen P, Tarkkanen M, Tanner M, Hakkarainen T, Kanerva A, Desmond RA, Pesonen S, et al. Oncolytic adenoviruses kill breast cancer initiating CD44+CD24-/low cells. Mol Ther 2007; 15:2088-93; PMID:17848962; http://dx.doi.org/10.1038/sj.mt.6300300

38. Kini LG, Herrero-Jimenez P, Kamath T, Sanghvi J, Gutierrez E Jr., Hensle D, Kogel J, Kusko R, Rexer K, Kurzweil R, et al. Mutator/hypermutable fetal/juvenile metakaryotic stem cells and human colorectal carcinogenesis. Front Oncol 2013; 3:267; PMID:24195059; http://dx.doi.org/10.3389/fonc.2013.00267